Benzene Oligocarboxylic Acids: Characterization by Isocratic, Linear Gradient, and Frontal Anion-Exchange Chromatography

Hong Li[1,*], **Leo Lue**[2,†], and **Costas S. Patrickios**[1,‡]

[1]Department of Chemical Engineering, University of Manchester Institute of Science and Technology (UMIST), P.O. Box 88, Manchester M60 1QD, U.K. and [2]Via Segaluzza 20, Pordenone, I-33170, Italy

Abstract

A series of nine benzene oligocarboxylic acids is characterized using anion-exchange chromatography to determine the steric mass-action affinity parameters: the characteristic charge, the equilibrium ion-exchange constant (and the corresponding Gibbs free energy of ion-exchange), and steric factor. Isocratic elution under various concentrations of sodium chloride in the mobile phase provides the characteristic charge and the ion-exchange constant. The former agrees closely with the number of carboxylic acid groups in the sample, and the latter seems to be strongly influenced by the relative positions of the carboxylic acid groups on the benzene ring. Analysis of all samples under a linear salt gradient provides retention times that follow the same order as the ion-exchange constants determined isocratically. Using an appropriate model, along with the isocratically determined characteristic charge and ion-exchange constant, the linear gradient retention times are predicted theoretically and agree well with the experimental times. Frontal experiments led to the calculation of the characteristic charge and the steric factor. The former agrees well with the value determined isocratically. For most samples, the steric factor increases slowly with the characteristic charge.

Introduction

Displacement chromatography emerges as a powerful tool for the preparative and analytical separation and concentration of pharmaceutical and nonpharmaceutical molecules (1–3). The current bottleneck for the transfer of displacement chromatography to the process scale is the lack of appropriate displacers. Originally, the focus was on high-molecular-weight (10,000–50,000) polymeric displacers (4,5) whose large number of functional groups ensured a successful displacement, but at the same time, makes their desorption for column regeneration more difficult. The finding that lower-molecular-weight (~2,000) polymeric displacers displayed sufficient affinity for the process (6) seemed to provide a solution to the problem of facile column regeneration. Recently, oligomeric (7–10) and monomeric (10,11) molecules have been identified as efficient displacers with even better characteristics with regard to their post-displacement removal.

In an effort to elucidate the critical structural features of the ion-exchange affinity of oligomeric compounds that may serve as displacers, a homologous family of seven α,ω-alkyl dicarboxylic acids was recently characterized (12). All homologues behaved similarly, displaying a low ion-exchange affinity (12). In the present study, isocratic, frontal, and linear salt gradient techniques were employed to comprehensively characterize a homologous family of nine benzene oligocarboxylic acids. Gerstner et al. (13) were the first to characterize the ion-exchange affinity of a relatively large number (five) of low-molecular-weight potential displacers. Their samples, however, did not belong to the same homologous series, because they comprised two amino acids and three oligopeptides. The present work constitutes a systematic screening of a large number (nine) of potential displacers belonging to the same homologous series. Most compounds in this investigation are commercially available at a relatively low cost and include homologues with different numbers of carboxylic acid groups and isomers with the same number of carboxylic acid groups but different relative positions of these groups within the benzene ring. The names and chemical structures of the dissociated forms of these compounds are shown in Figure 1. These molecules are easy to detect because of the high absorbance of the benzene ring in the ultraviolet (UV) region. Moreover, some of these compounds have proven to be nontoxic, such as benzoic acid, which is used as a food additive (14).

The most important finding is that the ion-exchange affinity of the characterized compounds is not solely defined by the number

*Current address: Department of Chemistry, University of Manchester, Oxford Road, Manchester M13 9PL, U.K.

† Current address: Physical and Chemical Properties Division, National Institute of Standards and Technology (NIST), 325 Broadway, Boulder, CO 80303-3328.

‡ Author to whom correspondence should be addressed: Department of Natural Sciences, School of Pure and Applied Sciences, University of Cyprus, P.O. Box 20537, 1678 Nicosia, Cyprus.

of functional groups but also by their geometrical arrangement (with the exception of the 1,3- and 1,4-dicarboxylic acids). For instance, it was determined that the ion-exchange constant of the hexa-substituted mellitic acid is lower than that of the symmetrically tri-substituted benzene 1,3,5-tricarboxylic acid, but higher than that of the tri-substituted benzene 1,2,3-tricarboxylic acid.

Experimental

Benzoic acid, phthalic acid, isophthalic acid, terephthalic acid, hemimellitic acid, trimellitic acid, trimesic acid, pyromellitic acid, mellitic acid, tris(hydroxymethylene) aminomethane (Tris), tris(hydroxymethylene) aminomethane hydrochloride (Tris HCl), sodium chloride, sodium nitrate, and a 0.5M sodium hydroxide solution were all purchased from Aldrich (Gillingham, Dorset, U.K.). Distilled, deionized water was used for the preparation of the mobile phases and the solutions of the samples. A Waters (Waterford, Herts, U.K.) analytical Protein-Pak Q 8HR strong anion-exchange column (100 × 5 mm) packed with 8-µm quaternary methylamine-derivatized beads of 100-nm average pore size was used for the experiments. The pH of the mobile phase was maintained at 8.0 using Tris buffer containing 28mM Cl^-. A Polymer Laboratories (Church Stretton, Shropshire, U.K.) LC1150 Quaternary Pump was used to deliver the solvent at a flow rate of 0.5 mL/min. A Polymer Laboratories LC1200 UV–visible detector was used to monitor the column effluent. An online Polymer Laboratories PL-DCU data collection unit and a computer were used for data acquisition. Solutions of the benzene oligocarboxylic acids at concentrations 10 mg/L were prepared by dissolving the solid sample (in the protonated form) in Tris buffer (pH 8.0) containing 28mM Cl^- and subsequently adjusting the pH to 8.0 by the addition of 0.5M NaOH solution

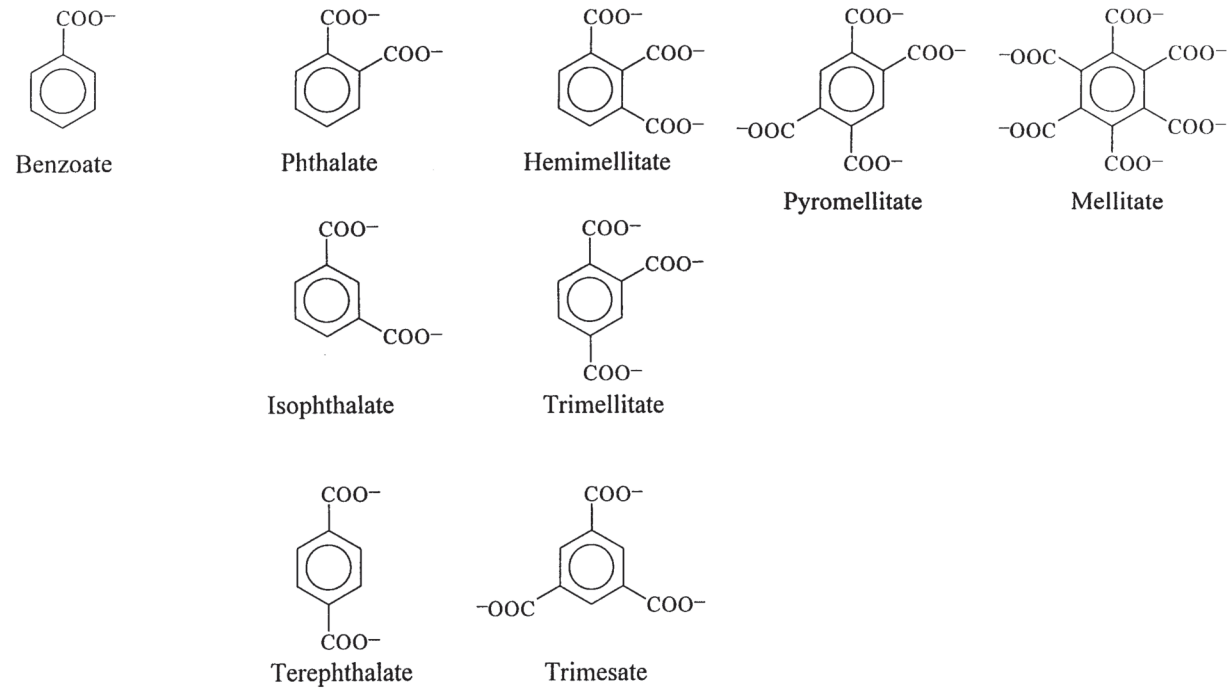

Figure 1. Chemical formulas and names of the nine benzene oligocarboxylic acids in the fully ionized state. The charge varies from 1 to 6. Isomers are placed in the same column.

Table I. Dissociation Constants of the Benzene Oligocarboxylic Acids*

Empirical name	IUPAC name	pK^{I}	pK^{II}	pK^{III}	pK^{IV}	pK^{V}	pK^{VI}
Benzoic	benzenecarboxylic	4.17	–	–	–	–	–
Phthalic	1,2-benzenedicarboxylic	2.98	5.28	–	–	–	–
Isophthalic	1,3-benzenedicarboxylic	3.46	4.46	–	–	–	–
Terephthalic	1,4-benzenedicarboxylic	3.51	4.82	–	–	–	–
Hemimellitic	1,2,3-benzenetricarboxylic	2.80	4.20	5.87	–	–	–
Trimellitic	1,2,4-benzenetricarboxylic	2.52	3.84	5.20	–	–	–
Trimesic	1,3,5-benzenetricarboxylic	3.12	3.89	4.70	–	–	–
Pyromellitic	1,2,4,5-benzenetetracarboxylic	1.92	2.87	4.49	5.63	–	–
Mellitic	1,2,3,4,5,6-benzenehexacarboxylic	1.40	2.19	3.31	4.78	5.89	6.96

* Taken from Reference 16.

when necessary.

Isocratic and gradient elution

A 7125 Rheodyne (Rohnert Park, CA) injector was used to introduce 20 µL of sample. The absorbance was monitored at 290 nm. In the isocratic experiments, the mobile phase chloride concentrations covered the range from 178 to 528mM by online mixing the appropriate proportions of two Tris buffer solutions (pH 8.0), one with 1.0M NaCl and the other without any salt added. In the gradient experiments, a linear 10-min gradient from 0.1 to 1.0M NaCl was applied at a flow rate of 0.5 mL/min. The gradient delay due to the dwell volume was 1.4 min, and the dead time of the column was 2.5 min at this flow rate.

Frontal experiments

A 10-port C10W Valco (Valco Instruments, Houston, TX) injection valve, fitted with one 5-mL loop and one 10-mL loop, was used to introduce the solutions of the samples.

Measurement of the column capacity

The column capacity in monovalent anions was measured by passing a front of 100mM sodium nitrate at 0.5 mL/min through the equilibrated (with buffer) column and determining the nitrate breakthrough time. The absorbance was monitored at 240 nm.

Isotherm determination

The adsorption isotherms of benzene 1,3,5-tricarboxylic acid and phthalic acid were determined by loading a range of sample concentrations onto the column and calculating the adsorbed amount from the breakthrough volume. Unlike the method of Jacobson et al. (15), the column was regenerated using a solution of 1M NaCl in the buffer and reequilibrated with salt-free buffer before a new concentration was loaded. The column effluent was monitored at 295 nm.

Determination of the steric factor and characteristic charge

A sequence of four frontal experiments was performed to calculate the steric factor and the characteristic charge of each sample. First, a front of the sample solution in the Tris buffer at pH 8.0 was passed through the column to saturate it and determine the amount of sample adsorbed from the breakthrough time. Second, with the polymer adsorbed, a front of 30mM sodium nitrate solution in pure water was introduced to calculate the amount of nitrate adsorbed, which corresponds to the number of column sites inaccessible to the sample. Third, a solution of 1M NaCl in the equilibration buffer was introduced to desorb the sample and regenerate the column. Fourth, the column was reequilibrated with the buffer.

Results and Discussion

All experiments in this study were performed at pH 8, where all carboxylic acid groups of all samples are fully dissociated. Table I lists the dissociation constants (p*K*s) of the benzene oligocarboxylic acids, which range from 1.4 to 7.0 [16].

Isocratic elution

The retention times (t_R) of the samples determined under isocratic elution conditions were converted to retention (or capacity) factors (k') using the following formula (17):

$$k' = (t_R - t_0)/t_0' \qquad \text{Eq. 1}$$

where t_0 is the dead time of the column, which is the elution time of an unretained solute, and t_0' is the column dead time corrected for non-column volume. The retention factors and the corresponding salt concentrations (C_{salt}) were combined to calculate the characteristic charge ν and the equilibrium ion-exchange constant K from the following equation (18–20):

$$\log k' = \log(\beta^n K \Lambda^n) - \nu \log C_{salt} \qquad \text{Eq. 2}$$

where β and Λ are the column phase ratio and column capacity in monovalent anions, respectively. The value of β was taken to be 0.5518 mL stationary phase/1 mL mobile phase, and the value of Λ was calculated from the nitrate capacity to be 487mM, in agreement with previous reports (4,21). Equation 2 describes Brooks and Cramer's (18) theory of steric mass action (SMA) ion-exchange under linear adsorption conditions with incorporation of the correction of Patrickios and Yamasaki (19,20).

The ion-exchange free energy ($\Delta G^{exchange}$) was calculated from K using the following equation (18):

$$\Delta G^{exchange} = -RT \ln K \qquad \text{Eq. 3}$$

where R is the gas constant, and T is the absolute temperature.

Figure 2 compares the characteristic charge of the nine molecules as calculated from the isocratic experiments with the corresponding number of carboxylic acid groups. The same figure also shows the characteristic charge calculated from the frontal experiments, which will be discussed later. The value of the isocratic characteristic charge (as well as that of the frontal characteristic charge) agrees closely with the number of dissociated carboxylic acid groups, because the points in the figure are

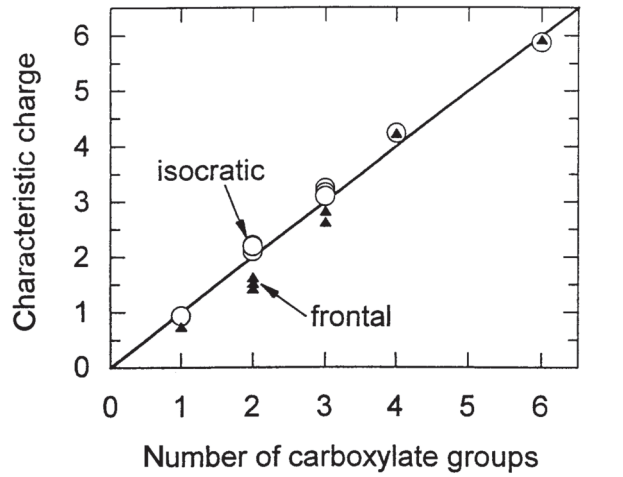

Figure 2. Dependence of the characteristic charge as determined by two different methods, isocratic elution (1) and frontal experiments (s), on the number of carboxylate groups in the benzene oligocarboxylates.

located very close to the line of unit slope passing from the origin. This implies that, upon adsorption, all carboxylate groups contact the surface, forming ionic bonds with the oppositely charged quaternary methylamine groups. It is not surprising that all functional groups of the benzene oligocarboxylic acids can exchange, given the flat shape of the benzene scaffold. In contrast, dendritic molecules characterized using similar techniques were found to contact the chromatographic surface using only a limited fraction (31–43%) of their functional groups, which are distributed evenly over their spherical outer surface (8). Figure 2 also reveals that within a group of isomers (i.e., the benzene dicarboxylates and tricarboxylates), the characteristic charge is practically unchanged.

Figure 3 displays the Gibbs free energy of ion-exchange ($\Delta G^{exchange}$) plotted against the characteristic charge (ν), both calculated from the isocratic experiments. The points in the figure are widely scattered. No clear monotonic dependence of $\Delta G^{exchange}$ with respect to ν is observed. It appears that a higher characteristic charge does not always imply a more negative free energy of ion-exchange. In fact, mellitate with six charges has a less favorable free energy of ion-exchange than the monovalent benzoate. Moreover, great differences between the free energy of ion-exchange of isomers are observed (with the exception of isophthalate and terephthalate). Note that no differences in the characteristic charges of the various isomers were observed in Figure 2. It appears that a higher charge density has an adverse effect on the free energy of ion-exchange of the isomers. For instance, focusing on the benzene dicarboxylates, it can be seen that the 1,2-isomer, the phthalate, has the lowest affinity. This molecule has the least favorable free energy of ion-exchange of all nine samples, presenting a positive value of $\Delta G^{exchange}$, indicating that the thermodynamically favored state is to remain in solution rather than to bind onto the chromatographic surface (with reference to the distribution of chloride counterions). 1,2,3-Tricarboxylate presents a near-zero value of $\Delta G^{exchange}$, whereas the rest of the samples display negative values of $\Delta G^{exchange}$.

Table II. Spacings Between the Carboxylate Groups in the Samples

Positions	Distance	Distance (pm)
1,2	*b*	370
1,3	$b\sqrt{3}$	641
1,4	2*b*	740

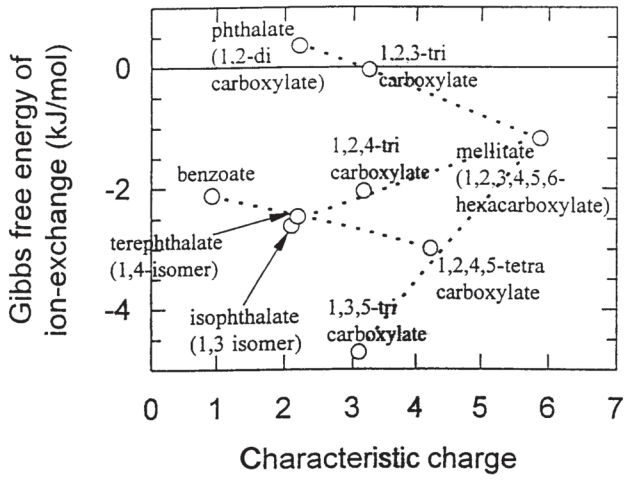

Figure 3. Dependence of the Gibbs free energy of ion-exchange on the characteristic charge, both determined from isocratic experiments. There are four groups of compounds that fall on straight (dotted) lines, indicating similarities in their ion-exchange characteristics.

Careful examination of Figure 3 can lead to the identification of four families of points that fall on straight lines indicated by dots in the figure (the trivial cases of the two vertical straight lines are ignored). We suggest that the species that fall on the same straight line share common characteristics in their ion-exchange behavior. The four families are as follows: (*a*) 1,2-dicarboxylate–1,2,3-tricarboxylate–1,2,3,4,5,6-hexacarboxylate, (*b*) benzoate–1,4-dicarboxylate and 1,3-dicarboxylate–1,2,4,5-tetracarboxylate, (*c*) 1,4-dicarboxylate and 1,3-dicarboxylate–1,2,4-tricarboxylate–1,2,3,4,5,6-hexacarboxylate, and (*d*) 1,3,5-tricarboxylate–1,2,4,5-tetracarboxylate–1,2,3,4,5,6-hexacarboxylate.

The first two groups exhibit a decrease in $\Delta G^{exchange}$ with ν, in agreement with the expectation that a greater number of charges in a sample would make its attraction to an oppositely charged surface more favorable. Surprisingly, the last two groups show exactly the opposite trend: a greater ν results in a less favorable $\Delta G^{exchange}$. This clearly implies the involvement of other interactions, in addition to the electrostatic attraction between the carboxylate groups of the sample to the oppositely charged quaternary methylamine groups of the surface, in the ion-exchange of the benzene oligocarboxylates. These other interactions may include steric hindrances, adsorbate–surface misregister, and binding of counterions to the sample in solution.

To explain this data, various scenarios were examined. To keep things simple, it was assumed that only two main factors dictate the trends in $\Delta G^{exchange}$. First, the possibility that the trends in free energy of ion-exchange were due to a combination of the number of charged groups in the samples and the proximity of these groups to the oppositely charged surface groups upon adsorption was investigated. Regarding the former, it was known that all carboxylic acid groups of all samples were fully ionized (from the p*K* values), and they all contacted the surface (from the characteristic charge values). Regarding the latter, molecular models of all samples and of the surface were constructed. The geometries of the molecular models are described below.

The benzene oligocarboxylate samples were assumed to have hexagonal geometry. The benzene ring was considered flat, and the plane of the carboxylate groups was considered vertical to the plane of the benzene ring. The bond lengths were taken as follows: C=C, 134 pm; C–C, 154 pm; C=O, 122 pm; C–O, 144 pm. The angle of O=C–O$^-$ was 109.5°. Based on this, the distance between two adjacent carboxylate groups (1,2-position) on the sample was estimated to be b = 370 pm. The distances between pairs of carboxylate groups at the 1,3- and 1,4-positions were also calculated and are presented in Table II.

In the absence of surface heterogeneity data, the adsorbing surface was assumed to be a square lattice with one point charge at each vertex of the square. Because the chromatographic surface is a functional polymethacrylate, the length of the side of the square was taken equal to the length of the methacrylate monomer repeat unit of α = 254 pm. This value of α is also consistent with

the manufacturer's specifications of specific surface area and column capacity, which lead to the calculation of one charged surface group per 6.25 $Å^2$ = (2.5 Å)^2 = (250 pm)^2. Table III shows the distances of the 11 closest neighbors on the square lattice, both in multiples of α as well as in picometers. These distances refer to diagonally placed neighbors (e.g. 1 × 1) as well as to neighbors placed along the same horizontal (or vertical) line (e.g. 1 × 0, 2 × 0).

Examination of the distances shown in Tables II and III suggests that the relative spacings cannot explain the trends in the free energies of ion-exchange. For instance, the less favorable experimental free energy of ion-exchange of the phthalate compared to that of the isophthalate would imply a poorer matching of the carboxylates of the phthalate with the surface groups in comparison with the isophthalate. Examination of the numbers in Tables II and III reveals that the phthalate can register to the surface groups better than the isophthalate. In particular, the best match of the two carboxylates of the phthalate, separated at 370 pm, is with two diagonally placed surface groups separated from each other at a distance of 359 pm. The best match for the isophthalate is less perfect; the two carboxylates of this sample, separated from each other at a distance of 641 pm, can register with two diagonally spaced surface groups separated by a distance of 568 pm from each other. Thus, the geometrical matching of the sample groups to the surface groups is not a major factor for the affinity of ion-exchange.

Table III. Spacings Between the Quaternary Methylamine Groups on the Surface

Spacing	Distance	Distance (pm)
1 × 0	α	254
1 × 1	α √2	359
2 × 0	2α	508
1 × 2	α √5	568
2 × 2	α √8	718
3 × 0	3α	762
1 × 3	α √10	803
2 × 3	α √13	916
4 × 0	4α	1016
1 × 4	α √17	1047
3 × 3	α √18	1078

Table IV. Educated Choices of the Number of Tightly Bound Sodium Ions to Benzene Oligocarboxylates in Solution

Sample name	Position of carboxylates	Number of bound sodium ions (ψ)
Benzoate	1	0
Phthalate	1,2	1
Isophthalate	1,3	0
Terephthalate	1,4	0
Hemimellitate	1,2,3	1.5
Trimellitate	1,2,4	1
Trimesate	1,3,5	0
Pyromellitate	1,2,4,5	1*
Mellitate	1,2,3,4,5,6	3

* Originally assigned a value of 2, consistent with the presence of two pairs of adjacent carboxylates in this sample; however, we subsequently observed that the quality of the fit in the linear regression was improved remarkably if a value of 1 was assigned.

In the second scenario, we hypothesized that the trends in $\Delta G^{exchange}$ are due to the following two factors: the number of charged groups in the samples, and the ability of the samples to complexate in solution with sodium cations; if a sample binds sodium more tightly than its isomer, then the former will be less likely to adsorb onto the ion-exchange surface than the latter. It was found that this hypothesis can explain the present data. Based on the observation that the samples with adjacent carboxylate groups have the least favorable Gibbs free energy of ion-exchange, it was assumed that these samples would bind sodium ions in solution more tightly than the others. This assumption is also consistent with information given in textbooks on inorganic chemistry, where the binding of alkali metal ions to salicaldehyde (a phenol with an aldehyde group at the *ortho-* position) is reported (22,23). It is known that alkali metal ions do not easily form complexes with organic ligands, because they do not have low-energy empty orbitals (22). They only complexate with strong multidentate ligands whose size is complementary to that of the alkali metal ions. Characteristic examples of such ligands are crown ethers and cryptands (22).

Next, it was assumed that the number of sodium ions that can bind tightly to the samples in solution varies between one (for the phthalate) and three (for the mellitate). Thus, as a first approximation, we considered that each independent pair of adjacent carboxylates binds to one sodium cation. Based on this, Table IV was constructed, and it shows educated choices for the number of tightly bound sodium ions to benzene oligocarboxylates in solution. Four of the samples were assigned zero tightly bound sodium ions, because they have zero pairs of adjacent carboxylate groups. Hemimellitate (1,2,3-tricarboxylate) with 3 adjacent carboxylates was assigned only 1.5 rather than 2 tightly bound sodium ions, because the 3 carboxylates do not form 2 independent pairs of carboxylates. This choice is also consistent with the 3 tightly bound sodium ions assigned for mellitate, possessing 6 adjacent carboxylates. A special case was presented by pyromellitate (1,2,4,5-tetracarboxylate), which should have been assigned 2 tightly bound sodium ions because of the 2 independent pairs of adjacent carboxylates. The assignment of only 1 tightly bound sodium ion for this sample was motivated by observation that a mathematical fit (see below) of our data was dramatically improved by adopting this choice. Indeed, it might be that this sample complexates in solution with only 1 sodium ion, which coordinates with the 2 symmetrically placed pairs of carboxylate groups. This choice of the number of tightly bound sodium ions to this sample in solution is consistent with the linearity of the points of the samples of family 4 in Figure 3: 1,3,5-tricarboxylate–1,2,4,5-tetracarboxylate–1,2,3,4,5,6-hexacarboxylate (discussed later).

It must be pointed out that it is quite possible that the number of solution-bound sodium ions varies between 2 (for the phthalate) and 6 (for the mellitate), rather than between 1 and 3. Indeed, this postulate would be more consistent with a stoichiometric displacement model (or, more simply, an electroneutrality condition) in solution. The reason why we proposed a 2:1

ratio of carboxylate groups to sodium ions in the previous paragraph is the precedent in the literature (22,23) that multifunctional chelators, such as crown ethers and cryptands, complexate to substoichiometric amounts of ions (the amount of bound ions corresponds to only a fraction, 10–50%, of the equivalence point).

A linear regression was then performed on the $\Delta G^{exchange}$ data to calculate the two contributions to the Gibbs free energy of ion-exchange: that due to the ion-exchange of individual carboxylate groups ($\Delta G^{carboxylate}$) and that due to the solution complexation of sodium ions to (more than half of) the samples (ΔG^{sodium}). The independent variables in the regression were the characteristic charge ν and the number of tightly bound sodium ions in solution (ψ). Thus, the relevant equation is as follows:

$$\Delta G^{exchange} = \nu\, \Delta G^{carboxylate} + \psi\, \Delta G^{sodium} \qquad \text{Eq. 4}$$

Due to the uncertainties in the estimated values of ψ, the values of ν used here were rounded to the nearest integer (which made them exactly equal to the number of carboxylate groups in the sample). The calculated values of the two contributions to the Gibbs free energy of ion-exchange and the corresponding 95% confidence intervals are $\Delta G^{carboxylate} = -1.46 \pm 0.24$ kJ/mol and $\Delta G^{sodium} = +2.65 \pm 0.61$ kJ/mol.

In both cases, the 95% confidence intervals are better than 25%. This is encouraging and supports the correctness of the hypothesis of this scenario. The algebraic signs of the two parameters are in agreement with expectations: the negative sign of $\Delta G^{carboxylate}$ indicates that the presence of more carboxylate groups enhances sample affinity for the surface, and the positive sign of ΔG^{sodium} suggests that the tight solution binding of more sodium ions to the samples reduces sample affinity for the surface. The absolute value of ΔG^{sodium} is almost double that of $\Delta G^{carboxylate}$, which can explain the diminished importance of the number of charged groups for the $\Delta G^{exchange}$ of some samples, such as the mellitate (Figure 3).

Should the number of bound sodium ions be varied between 2 and 6, the value of the calculated ΔG^{sodium} would be halved to 1.32 kJ/mol and be very close to the (absolute) value of $\Delta G^{carboxylate}$ of 1.46 kJ/mol. However, it is not believed that this proximity in values necessarily suggests the correctness of this modified scenario over the original scenario.

Figure 4 compares the experimental $\Delta G^{exchange}$ with those calculated using the above model. The agreement is satisfactory because the data points are distributed close to the straight line of unit slope passing from the origin. Given the satisfactory performance of the model with regard to the experimental data, we now go back to explain the straight lines passing from the four families of points in Figure 3. It is suggested that the samples that fall on the same straight line have their ψ and ν correlated through a linear equation of the following form:

$$\psi = m_i\, \nu + c_i \qquad \text{Eq. 5}$$

where m_i and c_i are constants describing a family of samples. Different families have different values of m_i and c_i. The values of ψ listed in Table IV were used along with the rounded values of ν to calculate the m_i and c_i for each of the four families. Linear regression gave the results shown in Table V. ψ is plotted against ν in Figure 5, where the straight lines with slope m_i and intercept c_i are also shown. The fits are very good, except perhaps the one for family 2, for which the correlation coefficient (also shown in

Table V. Values of m_i and c_i*

Family	Family members	Slope m_i	Intercept c_i	Correlation coefficient
1	(1,2), (1,2,3), (1,2,3,4,5,6)	0.50	0.00	1.0000
2	(1), (1,4), (1,3), (1,2,4,5)	0.37	–0.58	0.9272
3	(1,4), (1,3), (1,2,4), (1,2,3,4,5,6)	0.74	–1.42	0.9961
4	(1,3,5), (1,2,4,5), (1,2,3,4,5,6)	1.00	–3.00	1.0000

* Calculated using the values of ψ shown in Table IV.

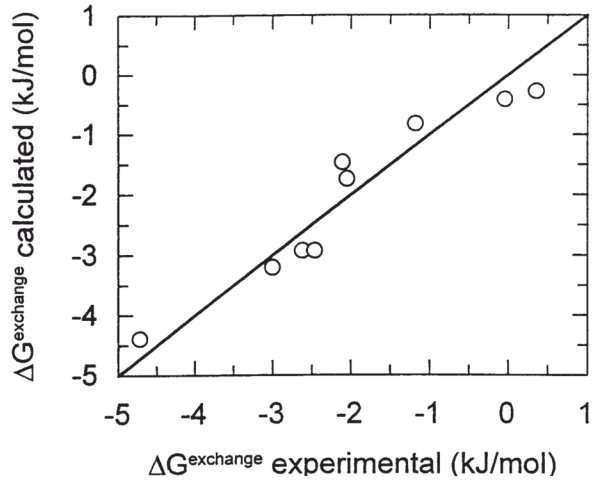

Figure 4. Comparison between calculated and experimental Gibbs free energy of ion-exchange of benzene oligocarboxylates. This model is based on the assumption that the Gibbs free energy of ion-exchange depends linearly on two variables: first, the number of carboxylate groups, and second, the number of independent pairs of adjacent carboxylate groups.

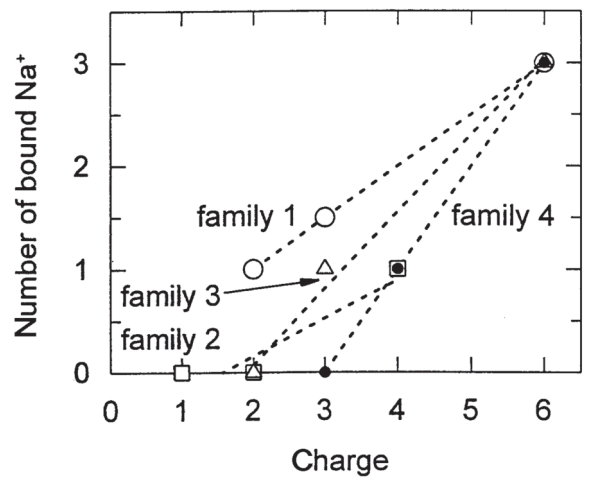

Figure 5. Dependence of the number of independent pairs of adjacent carboxylate groups (leading to the solution complexation of an equivalent number of sodium ions) on the number of carboxylate groups on benzene oligocarboxylates. The samples fall on four straight lines defining four families. This explains the four straight lines of Figure 3.

Table V) is relatively low (0.93).

Substituting Equation 5 into Equation 4, the following equation is obtained:

$$\Delta G^{exchange} = \nu \left(\Delta G^{carboxylate} + m_i \Delta G^{sodium} \right) + c_i \Delta G^{sodium} \quad \text{Eq. 6}$$

which suggests that, within a family of samples, $\Delta G^{exchange}$ is a linear function of ν, thus explaining the linearities observed in Figure 3.

The bare and hydrated diameters of sodium ions are 190 and 720 pm, respectively (24), which must be compared with the (1,2), (1,3), and (1,4) spacings of benzene oligocarboxylates of 370, 641, and 740 pm, respectively (Table II). If the adsorbed sodium ions lie in the space between the two adjacent carboxylates (as opposed to a nonlinear triangular arrangement), then the adsorbed sodium ions must be dehydrated. Moreover, if we take into account the finite volume of the oxygen atom of the carboxylate group that has a radius of approximately 100 pm, then the free space in the (1,2) cavity is (370 – 2 × 100) pm ≅ 170 pm, which matches very well the sodium ion bare diameter of 190 pm. It would be interesting to repeat some of these isocratic experiments replacing Na^+ with different solution counterions, such as Li^+, K^+, or Cs^+. These cations have bare diameters ranging from 136 to 338 pm (24), and their utilization should affect the ion-exchange behavior of benzene oligocarboxylates. A more drastic test can be the replacement of Na^+ by a bulky organic cation, such as tetramethylammonium with a bare diameter of 694 pm (24).

Our interpretation of the data suggests that a higher charge density of the sample leads to a lower ion-exchange affinity because of strong binding of counterions in solution. This result should be considered when examining the ion-exchange affinities of protein variants with the same number of electrostatically binding groups distributed in various ways on the protein surface. The conventional explanation for these studies has been that the more strongly retained variants possess charge patches (i.e., higher charge densities) (25,26). The present work implies that this explanation must be reexamined. We recognize, however, that due to the larger size and three-dimensional structure of proteins, protein adsorption behavior is more complicated than that of small molecules, such as benzene oligocarboxylic acids. Thus, the conclusion drawn regarding the charge density and adsorption affinity of our solutes should be exported to proteins with caution.

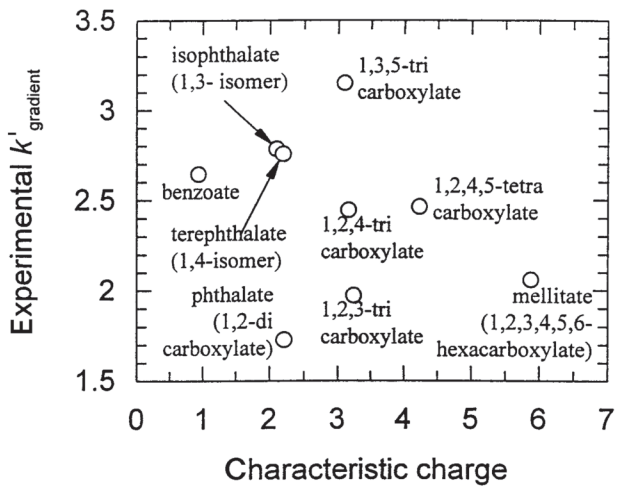

Figure 6. Dependence of the retention (capacity) factors measured under a linear salt gradient on the characteristic charge of benzene oligocarboxylates. The trends are the same as those of the Gibbs free energy of ion-exchange versus characteristic charge depicted in Figure 3.

Our conclusion of solution counterion binding can be used to explain the relative ion-exchange affinities of oligoamine-based cationic displacers, recently determined by Cramer et al. (27,28). These investigators reported that a macrocyclic tetra-amine has a lower affinity (in terms of its $\Delta G^{exchange}$) than its linear analogue. The explanation we propose for this is that the former molecule forms more stable complexes with counterions in solution than the linear tetra-amine, leading to a weaker surface-adsorption tendency of the macrocycle; this solution complexation behavior is also documented in the literature (23).

Gradient elution

The elution of the benzene oligocarboxylates under a linear salt gradient was studied, and the retention times were measured, from which the retention (capacity) factors were calculated from Equation 1. These retention factors (k') are plotted against the isocratically determined characteristic charge ν in Figure 6. The trends in this figure are very similar to those in Figure 3.

Brooks and Cramer's (18) affinity theory can predict the retention times in ion-exchange gradient elution of a solute, given its characteristic charge and ion-exchange constant [29]. It was therefore decided to calculate the gradient retention factors of the benzene oligocarboxylates using the theory and the isocratically determined characteristic charge and ion-exchange constant, and the results were compared with the experimentally determined gradient retention factors. This comparison tested Brooks' theory and the consistency of our isocratic and gradient experimental methods.

For the prediction of the linear gradient retention factors, an equation initially developed by Cramer et al. (29) was used after appropriate modification to include the gradient delay time (t_d) and the correction of Patrickios and Yamasaki (19). The following expression is the equation developed for the present calculations, which provides the linear gradient retention factor k' as a function of K and ν:

$$k' = \frac{t_d}{t_0} + \frac{1}{G}\left\{\left[(\nu+1)G\left(K\beta^n\Lambda^n - \frac{t_d}{t_0}C_0^n\right) + C_0^{n+1}\right]^{\frac{1}{\nu+1}} - C_0\right\} \quad \text{Eq. 7}$$

where G is the gradient's slope given by the following:

$$G = (C_F - C_0)/(t_G/t_0) \quad \text{Eq. 8}$$

t_G is the duration of the salt gradient and C_0 and C_F are the gradient's initial and final salt concentrations.

The calculated k' values are compared with the experimental ones in Figure 7. Although the predicted values are generally lower than the experimental values, the agreement is satisfactory because the points lie close to the straight line of unit slope passing from the origin. The success of the prediction supports the validity of Brooks' theory and also suggests that the present two experimental techniques, the linear gradient and isocratic

elutions, are mutually consistent.

Frontal Experiments

Isotherms

Figure 8 shows the adsorption isotherms for the most weakly and most strongly retained samples, phthalate (1,2-benzene dicarboxylate) and trimesate (1,3,5-benzene tricarboxylate), respectively. The isotherm of the trimesate is practically square (very steep) for the concentrations investigated. The isotherm of the phthalate is more curved, reflecting its lower affinity for the surface. The small arrows in the two isotherms indicate mobile phase concentrations of 1% (w/v); this is the concentration at which the frontal experiments described in the previous part of the paper were performed. Both arrows lie in the horizontal part of the isotherms where the column is saturated with the sample. The phthalate isotherm lies above the trimesate isotherm because a greater number of molecules of the former can be accommodated in a given column area due to its lower characteristic charge than that of trimesate (this statement assumes similar values of the steric factors of the two solutes; see following section).

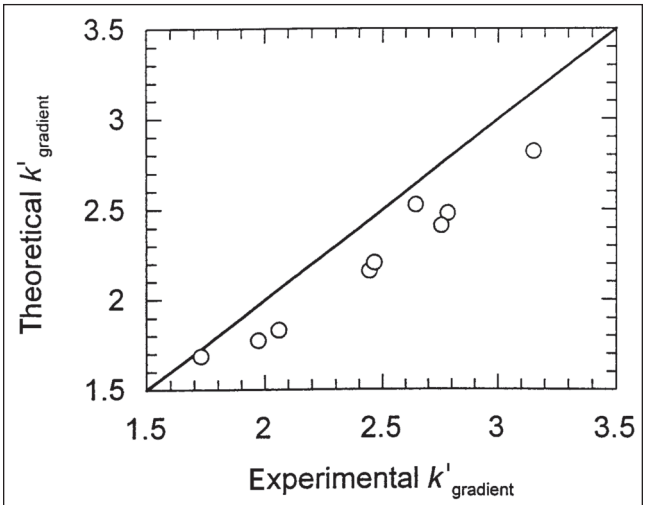

Figure 7. Comparison between the experimental linear gradient retention factors and the independently predicted linear gradient retention factors. The prediction utilized the isocratically determined characteristic charges and ion-exchange constants.

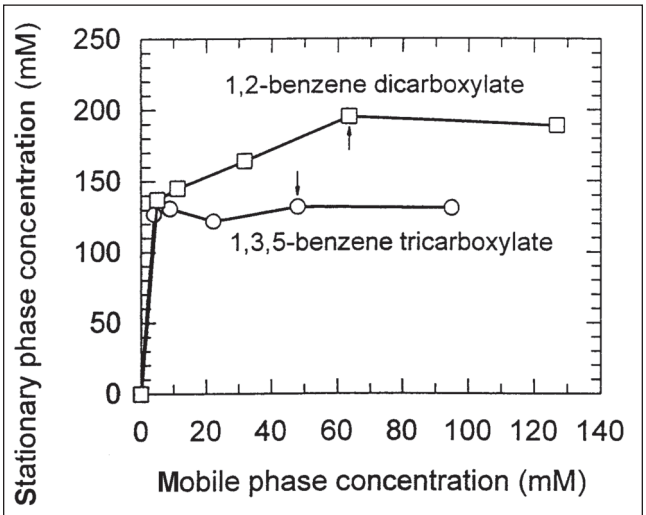

Figure 8. Adsorption isotherms of the two benzene oligocarboxylates with extreme Gibbs free energies of ion-exchange: 1,3,5-benzene tricarboxylate (trimesate) with the most favorable Gibbs free energy of ion-exchange and 1,2-benzene dicarboxylate (phthalate) with the least favorable. Both species, but in particular the former, present practically square adsorption isotherms for the concentration range investigated.

Frontal characteristic charge and steric factor

The stationary phase concentrations of all samples were measured by loading 1% (w/v) solutions onto the column and measuring the breakthrough volumes. The results of the previous paragraph suggest that a 1% (w/v) mobile phase sample concentration is sufficient to saturate the stationary phase. Column saturation means that no more sample molecules can be adsorbed, but it does not necessarily mean that all chloride surface counterions have been displaced by the sample. The bulkiness of the sample may sterically hinder some surface sites, which then become inaccessible for exchange (18). These sterically hindered sites were measured by introducing a low (to avoid sample displacement or desorption) concentration sodium nitrate front in the presence of the adsorbed benzene oligocarboxylate, which causes the exchange of the chlorides occupying the inaccessible sites (4).

The steric factor σ, defined as the number of sterically hindered column sites per adsorbed sample molecule at column saturation, was calculated:

$$\sigma = \frac{\text{(number of moles of nitrate adsorbed in the presence of the adsorbed sample)}}{\text{(number of moles of sample adsorbed)}} \quad \text{Eq. 9}$$

The "frontal" characteristic charge ($\nu_{frontal}$), defined as the number of column sites occupied by the sample per adsorbed sample molecule, was calculated:

$$\nu_{frontal} = \frac{\text{[(total number of moles of column surface sites) – (number of moles of nitrate adsorbed)]}}{\text{(number of moles of sample adsorbed)}} \quad \text{Eq. 10}$$

where the total number of moles of column surface sites are measured with another nitrate front in the absence of adsorbed benzene oligocarboxylate.

The values of $\nu_{frontal}$ determined from this calculation have been plotted in Figure 2 and agree well with the number of carboxylate groups in each sample. For the lower homologues (benzoate, dicarboxylates, and tricarboxylates), $\nu_{frontal}$ was slightly lower than ν determined isocratically. For the higher homologues (tetracarboxylate and hexacarboxylate), the values of $\nu_{frontal}$ closely matched those of ν.

Figure 9 shows σ plotted against $\nu_{frontal}$, both determined from the frontal experiments. σ increases slowly with $\nu_{frontal}$, reaching a value of 1.5 for the tetracarboxylate. The steric factor rises abruptly for the hexacarboxylate for which it acquires a value of 4.9. Simple geometric calculations can show that the surface area of a regular hexagon is double that of an equilateral triangle inscribed in the same circle. This would imply that, to a first approximation, the steric factor of the tricarboxylate should be

half that of the hexacarboxylate. Thus, the steric factor of the tricarboxylate should have been 2.5 rather than 1. The discrepancy can be rationalized by the fact that the tricarboxylate is a relatively small molecule and can more efficiently minimize the number of sterically shielded surface sites by rotating around its threefold axis and attaining the best (parallel) orientation relative to the square lattice of the adsorbing surface. This was confirmed by molecular model construction, which showed that when adsorbed onto the surface, the hexacarboxylate shields four surface sites, whereas the other samples at the optimal orientation shield only 1–2 sites. Thus, the trends in the variation of the steric factor can be explained from the size of the sample and the charge density of the surface. Unfortunately, this conclusion cannot be compared with the results of other workers, because the few relevant studies (4,7,8) did not attempt to relate the steric factors and characteristic charges of their oligo- or poly-electrolytes to solute geometry and surface group placement.

Conclusion

A comprehensive experimental study of the anion-exchange characterization of nine benzene oligocarboxylic acids was presented. The techniques comprised isocratic, linear gradient, and frontal elution. The values of characteristic charge determined from the isocratic and frontal experiments suggest that all carboxylic acid groups of all samples bind to the surface, which is consistent with the flat shape of the benzene scaffold and the relatively high pH that ensures ionization of all carboxylic acid groups of all samples. The isocratically determined Gibbs free energies of ion-exchange seem to have two contributions: one from the number of ionized carboxylic acid groups, and one from the number of solution bound counterions promoted by the presence of adjacent carboxylates. The experimental linear gradient retention factors were accurately reproduced using a theoretical model along with the independently determined (from the isocratic experiments) characteristic charge and Gibbs free energy of ion-exchange. The adsorption isotherms of the samples are essentially square and become flat at 1% (w/v) mobile phase concentration. With the exception of benzene hexacarboxylate, the steric factor of the samples is rather low and increases slowly with the characteristic charge.

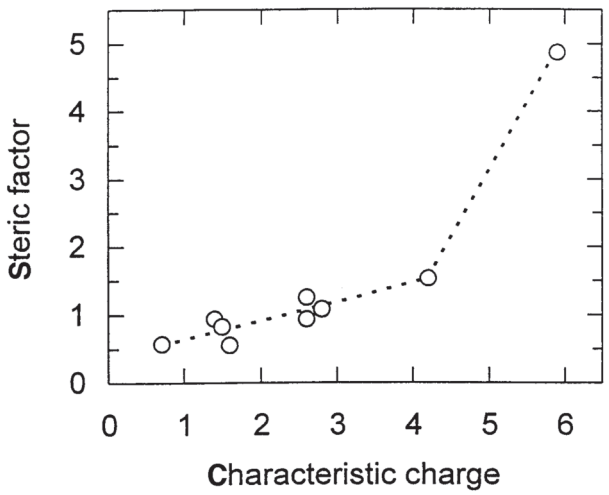

Figure 9. Dependence of the steric factor on the characteristic charge of the benzene oligocarboxylates, both determined by frontal elution. The dotted lines are not based on a model but are drawn to lead the eye.

Protein displacement experiments are underway. The samples with high characteristic charge and low Gibbs free energy of ion-exchange, in particular the 1,3,5-tricarboxylate, are expected to act as efficient displacers. It will also be interesting to examine the efficiency of benzene hexacarboxylate which, although displaying a relatively high Gibbs free energy of ion-exchange, has a high steric factor that will minimize the salt concentration in the induced front upon its adsorption, thus enhancing the quality of the separation.

Acknowledgments

The authors are grateful to the Biotechnology and Biological Sciences Research Council (BBSRC, U.K.) for the grant support (36/T0 7395) that enabled this work. The authors would also like to thank Dr. Lars Hagel of Pharmacia Biotech (Uppsala, Sweden) for kindly donating chromatographic media that were used in the beginning of the project.

References

1. R. Freitag. Displacement chromatography for biopolymer separation. *Nature Biotechnol.* **17:** 300–302 (1999).
2. J. Gerstner. Cleaner separations. *Chem. Br.* **February:** 40–42 (1997).
3. S.M. Cramer. Displacement chromatography. *Nature* **351:** 251–52 (1991).
4. S.D. Gadam, G. Jayaraman, and S.M. Cramer. Characterization of non-linear adsorption properties of dextran-based polyelectrolyte displacers in ion-exchange systems. *J. Chromatogr.* **630:** 37–52 (1993).
5. G. Jayaraman, S.D. Gadam, and S.M. Cramer. Ion-exchange displacement chromatography of proteins: dextran-based polyelectrolytes as high-affinity displacers. *J. Chromatogr.* **630:** 53–68 (1993).
6. S.C. David Jen and N.G. Pinto. Use of the sodium salt of poly(vinylsulfonic acid) as a low-molecular-weight displacer for the protein separations by ion-exchange displacement chromatography. *J. Chromatogr.* **519:** 87–98 (1990).
7. A. Kundu, S. Vunnum, and S.M. Cramer. Antibiotics as low-molecular-mass displacers in ion-exchange displacement chromatography. *J. Chromatogr. A* **707:** 57–67 (1995).
8. G. Jayaraman, Y.F. Li, J.A. Moore, and S.M. Cramer. Ion-exchange displacement chromatography of proteins: dendritic polymers as novel displacers. *J. Chromatogr. A* **702:** 143–55 (1995).
9. A. Kundu, A.A. Shukla, K.A. Barnthouse, J. Moore, and S.M. Cramer. Displacement chromatography of proteins using sucrose octasulfate. *BioPharm* **May:** 64–70 (1997).
10. A. Kundu, S. Vunnum, G. Jayaraman, and S.M. Cramer. Protected amino acids as novel low-molecular-weight displacers in cation-exchange displacement chromatography. *Biotechnol. Bioeng.* **48:** 452–60 (1995).
11. A. Kundu, K.A. Barnthouse, and S.M. Cramer. Selective displacement chromatography of proteins. *Biotechnol. Bioeng.* **56:** 119–29 (1997).

12. A.R. Khan and C.S. Patrickios. α,ω-Alkyl dicarboxylic acids: characterization by isocratic anion-exchange chromatography. *J. Chromatogr. Sci.* **37:** 150–54 (1999).
13. J.A. Gerstner, J.A. Bell, and S.M. Cramer. Gibbs free energy of adsorption for biomolecules in ion-exchange systems. *Biophys. Chem.* **52:** 97–106 (1994).
14. R.C. Lindsay. Food additives. In *Food Chemistry*, 3rd ed., O.R. Fennema, Ed. Marcel Dekker, New York, NY, 1996, pp 788–89.
15. J. Jacobson, J. Frenz, and C. Horváth. Measurement of adsorption isotherms by liquid chromatography. *J. Chromatogr.* **316:** 53–68 (1984).
16. G.D. Fasman. *Handbook of Biochemistry and Molecular Biology, Physical and Chemical Data,* Vol. I, 3rd ed. CRC Press, Cleveland, OH, 1976, p 313.
17. P.C. Wankat. *Rate Controlled Separations*. Elsevier Science, New York, NY, 1990.
18. C.A. Brooks and S.M. Cramer. Steric mass-action ion exchange: displacement profiles and induced salt gradients. *Am. I. Chem. Eng. J.* **38:** 1969–78 (1992).
19. C.S. Patrickios and E.N. Yamasaki. A correction to the calculation of the Gibbs free energy of adsorption for biomolecules in ion-exchange systems. *Biophys. Chem.* **69:** 219–20 (1997).
20. C.S. Patrickios and E.S. Patrickios. Stoichiometric mass-action ion-exchange model: explicit isotherms for monomeric, dimeric, trimeric and tetrameric ions. *J. Chromatogr. A* **694:** 480–85 (1995).
21. C.S. Patrickios, S.D. Gadam, W.R. Hertler, S.M. Cramer, and T.A. Hatton. Block methacrylic polyampholytes as protein displacers in ion-exchange chromatography. *Biotechnol. Prog.* **11:** 33–38 (1995).
22. J.D. Lee. *Concise Inorganic Chemistry*, 4th ed. Chapman & Hall, London, England, 1994, pp 305–308.
23. J. Burgess. *Ions in Solution: Basic Principles of Chemical Interactions*. Ellis Horwood, Chichester, England, 1988, pp 71–72, 80–83, 83–91.
24. J. Israelachvili. *Intermolecular & Surface Forces*, 2nd ed. Academic Press, London, England, 1991, p 55.
25. R.D. Johnson, R.J. Todd, and F.H. Arnold. Multipoint binding in metal-affinity chromatography. II. Effect of pH and imidazole on chromatographic retention of engineered histidine-containing cytochromes *c*. *J. Chromatogr. A* **725:** 225–35 (1996).
26. D.J. Roush, D.S. Gill, and R.C. Wilson. Preferred high-performance liquid chromatographic anion-exchange chromatographic contact region for recombinant rat cytochrome b_5. *J. Chromatogr. A* **704:** 339–49 (1995).
27. A.A. Shukla, K.A. Barnthouse, S.S. Bae, J.A. Moore, and S.M. Cramer. Structural characteristics of low-molecular-mass displacers for cation-exchange chromatography. *J. Chromatogr. A* **814:** 83–95 (1998).
28. A.A. Shukla, S.S. Bae, J.A. Moore, and S.M. Cramer. Structural characteristics of low-molecular-mass displacers for cation-exchange chromatography. II. Role of the stationary phase. *J. Chromatogr. A* **827:** 295–310 (1998).
29. S.R. Gallant, S. Vunnum, and S.M. Cramer. Optimization of preparative ion-exchange chromatography of proteins: linear gradient separations. *J. Chromatogr. A* **725:** 295–314 (1996).

Manuscript accepted September 30, 1999.